Inorganic Chemistry

ARTICLE

pubs.acs.org/IC

Synthesis and Characterization of the Phosphorus Triazides $OP(N_3)_3$ and $SP(N_3)_3$

Xiaoqing Zeng,*[,†] Eduard Bernhardt,[†] Helmut Beckers,[†] and Helge Willner[†]

[†]FB C — Anorganische Chemie, Bergische Universität Wuppertal, Gauss Strasse 20, D-42097 Wuppertal, Germany

Supporting Information

ABSTRACT: Two explosive triazides of phosphorus(V), $OP(N_3)_3$ and $SP(N_3)_3$, have been prepared as neat substances and structurally characterized. Both compounds can be handled in gas, liquid, and solid states in submillimolar quantities. The melting points of $OP(N_3)_3$ and $SP(N_3)_3$ are +22 and −30 °C, respectively. The two triazides have been characterized by IR (Ar matrix and gas phase) and Raman (solid) spectroscopies. Their single-crystal structures were obtained by X-ray diffraction and found to be significantly distorted from the predicted ideal C_3 symmetry because of intermolecular interactions. The spectroscopic and structural properties are discussed in combination with density functional theory calculations.

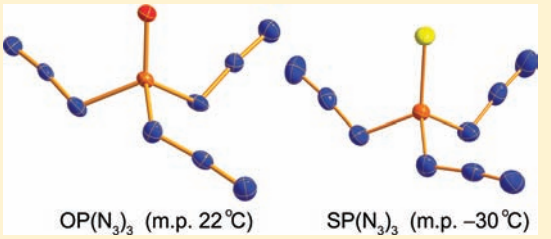

INTRODUCTION

Main-group covalent azides have been the targets of extensive experimental studies for more than a century, and some have been widely used in chemistry and biology.[1] As highly endothermic compounds, polyazides in a pure form are thermally unstable and, in some cases, are extremely heat- and shock-sensitive. These features mainly impede their isolation and structural characterization, although some of them had already been identified in solutions many years ago. However, with the development of new synthetic methods and particularly sophisticated experimental skills, more and more exciting covalent azides have been isolated and structurally characterized in recent years,[2] including the parent compound hydrazoic acid (HN_3), for which the solid-state structure has very recently been reported.[3]

Experimental studies of the neutral polyazides of group 15 heavy elements date back to the 1970s when the first spectroscopic characterizations (IR, Raman, and ^{31}P NMR) of $P(N_3)_3$, $OP(N_3)_3$, and $P(N_3)_5$ in organic solvents by Buder and Schmidt were performed,[4] but none have been structurally characterized. Thiophosphoryl triazide [$SP(N_3)_3$] has also been known since the 1970s as a manageable compound in CH_3CN solutions.[5] It found application as an in situ Staudinger reagent, but the neat compound has never been isolated.[6] Recently, much progress has been achieved in the synthesis and structural characterization of neutral binary polyazides of the heavier group 15 elements, including $As(N_3)_3$,[7] $As(N_3)_5$,[8] $Sb(N_3)_3$,[9] $Sb(N_3)_5$,[8] and $Bi(N_3)_3$.[10]

As a continuation of our interest in the structures,[11] matrix isolation, and chemistry[12] of covalent azides, we report herein the isolation of the two phosphorus triazides, $OP(N_3)_3$ and $SP(N_3)_3$, and their spectroscopic and structural characterization in combination with density functional theory (DFT) calculations.

EXPERIMENTAL SECTION

Caution! *Covalent azides are potentially hazardous and explosive. Because $OP(N_3)_3$ and $SP(N_3)_3$ are explosive compounds, they should be handled in submillimolar quantities only. Although we have not experienced any explosions during this work, safety precautions (face shields, leather gloves, and protective leather clothing) are strongly recommended. Scratching and breaking of ampules containing shock-sensitive azides by the ampule-key technique[13] can lead to explosions. All manipulations with the triazides must be done with appropriate safety precautions.*

Materials and Apparatus. Phosphoryl trichloride ($OPCl_3$, Merck) and thiophosphoryl trichloride ($SPCl_3$, Merck) were purified by fractional condensation, and their purity was checked by gas-phase IR spectroscopy before use. Sodium azide (NaN_3, Merck) was dried at 100 °C under vacuum before use. For the preparation of ^{15}N-labeled samples, 1-^{15}N sodium azide (98 atom % ^{15}N, EURISO-TOP GmbH) was used as received. Acetonitrile (CH_3CN, Merck) was dried with P_4O_{10} and distilled immediately before use. Reactions were performed in a glass vessel (volume 25 mL and length 20 cm) connected to the vacuum line and equipped with a small magnetic stir bar and a valve fitted with a poly(tetrafluoroethylene) (PTFE) stem (Young, London, U.K.). Volatile materials were manipulated in a glass vacuum line equipped with a capacitance pressure gauge (221 AHS-1000, MKS Baratron, Burlington, MA), three U-traps, and valves with PTFE stems. The vacuum line was connected to an IR gas cell (optical path length 20 cm, Si windows of 0.6 mm thickness), fitted into the sample compartment of the Fourier transform infrared (FT-IR) instrument (Bruker, Vector 22) for measuring gas-phase IR spectra at a resolution of 2 cm^{-1}. The purified products were stored in flame-sealed glass ampules in liquid nitrogen. Glass ampules were opened on the vacuum line using an ampule key.[13]

Synthesis of $OP(N_3)_3$. On the glass vacuum line, CH_3CN (1 mL) and $OPCl_3$ (0.5 mmol) were successively condensed into the reaction vessel, which was charged with dried NaN_3 (0.2 g, 3 mmol) and held at −196 °C. The vessel was warmed to room temperature and stirred for 2 days. The vessel was then slowly opened to the vacuum line, and all of the volatile products were directed through three cold traps held at −30, −100, and −196 °C. The product $OP(N_3)_3$ (ca. 50 mg) was retained in

Received: August 18, 2011
Published: September 29, 2011

the first trap as a white solid. Acetonitrile and traces of unreacted $OPCl_3$ were retained in the middle trap. Traces of noncondensed gas (probably nitrogen) at −196 °C were observed. The purity of the product was checked by its gas-phase IR spectrum.

Synthesis of $SP(N_3)_3$. The preparation of $SP(N_3)_3$ was performed in a manner similar to that of $OP(N_3)_3$. Sodium azide (0.2 g, 3 mmol), CH_3CN (1 mL), and $SPCl_3$ (0.5 mmol) were used. The reaction mixture was stirred at room temperature for 2 h, and the volatile products were passed through cold traps held at −45, −100, and −196 °C. The product, $SP(N_3)_3$ (ca. 70 mg), was retained in the first trap as a colorless supercooled liquid. Acetonitrile remained in the middle trap. Again some noncondensed gas (nitrogen gas) at −196 °C was observed. The purity of the product was checked by its gas-phase IR spectrum.

Spectroscopy. Low-temperature Raman measurements were performed using small amounts of sample (ca. 10 mg) condensed in vacuo onto a stainless steel coldfinger (−196 °C). The coldfinger was then rotated to allow the sample to be exposed to the laser beam. The Raman spectra were recorded on a Bruker-Equinox 55 FRA 106/S FT-Raman spectrometer using a 1064 nm Nd:YAG laser (150 mW) with 200 scans at a resolution of 2 cm^{-1}.

Matrix IR spectra were recorded on a FT-IR spectrometer (IFS 66v/S Bruker) in a reflectance mode using a transfer optic. A KBr beam splitter and a mercury−cadmium telluride (MCT) detector were used in the region of 4000−550 cm^{-1}. For each spectrum, 200 scans at a resolution of 0.25 cm^{-1} were coadded. The gaseous sample was mixed by passing a flow of argon gas through a U-trap containing ca. 10 mg of the azide, which was kept in a cold ethanol bath [−15 °C for $OP(N_3)_3$ and −27 °C for $SP(N_3)_3$]. When the flow rate of argon gas (2 mmol h^{-1}) was adjusted, a small amount of the resulting mixture (azide/Ar ≈ 1: 1000 estimated) was passed through a quartz furnace with a nozzle (diameter 1.0 mm) at a pressure of about 1 mbar, which can be electrically heated by a platinum wire (diameter 0.25 mm and length of the heated zone 10 mm). Then the mixture was deposited at a high vacuum onto the matrix support at 16 K (Rh-plated Cu block).

Single-Crystal Structure Determination. *a. Crystal Growth and Transfer.* A small amount (ca. 10 mg) of the sample was condensed (−196 °C) into the upper part of a glass container (o.d. 1 cm and length 15 cm), which was equipped with a valve with a PTFE stem and connected to the vacuum line. The lower part of the container (ca. 5 cm) was immersed in a cold bath overnight [0 °C for $OP(N_3)_3$ and −78 °C for $SP(N_3)_3$], while the upper part was slowly warmed to room temperature, and colorless crystals were obtained at the bottom. The container with the crystals was cooled in dry ice, connected to the vacuum line, filled with 1 atm of argon gas, and cut. The crystals were quickly poured into a trough that was precooled by a flow of cold nitrogen gas [−20 °C for $OP(N_3)_3$ and −40 °C for $SP(N_3)_3$]. Suitable crystals were subsequently selected under the microscope and mounted as previously described.[11]

b. Collection and Reduction of X-ray Diffraction Data. Crystals were mounted on an Oxford Diffraction Gemini E Ultra diffractometer, equipped with a 2K × 2K EOS CCD area detector, a four-circle κ goniometer, an Oxford Instruments cryojet, and sealed-tube Enhanced (Mo) and Enhanced Ultra (Cu) sources. For data collection, a Cu source emitting monochromated Cu Kα radiation (λ = 1.541 84 Å) was used. The diffractometer was controlled by *CrysAlisPro* Graphical User Interface software.[14] The diffraction data collection strategy was optimized with respect to complete coverage and consisted of 10 ω scans with a width of 1°, respectively. The data collection for $OP(N_3)_3$ and $SP(N_3)_3$ was carried out at −133 °C, in a 1024 × 1024 pixel mode using 2 × 2 pixel binning. Processing of the raw data, scaling of the diffraction data, and application of an empirical absorption correction was completed by using the *CrysAlisPro* program.[14]

c. Solution and Refinement of the Structure. The solution of the structure was performed by direct methods, which located the positions of all atoms. The final refinement was obtained by introducing anisotropic thermal parameters and the recommended weightings for all atoms. All calculations were performed using the *WinGX v1.64.05* package program for structure determination, solution refinement, and molecular graphics.[15−18]

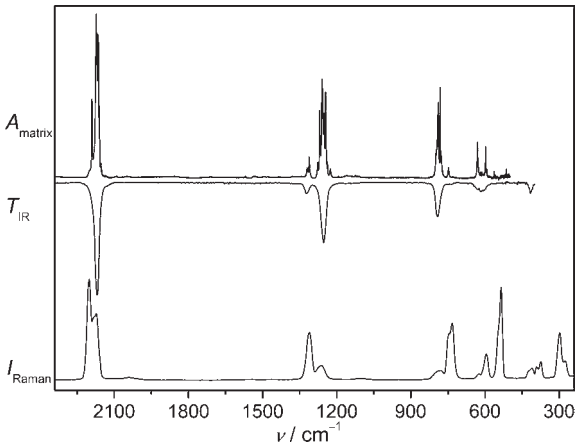

Figure 1. Upper trace: IR spectrum of $OP(N_3)_3$ isolated in an Ar matrix at 16 K (absorbance A, resolution 0.25 cm^{-1}). Middle trace: IR spectrum of gaseous $OP(N_3)_3$ at 298 K (transmission T, resolution 2 cm^{-1}). Lower trace: Raman spectrum of solid $OP(N_3)_{32}$ at 77 K (Raman intensity I, resolution 2 cm^{-1}).

Computational Details. Structures were optimized using the DFT-B3LYP[19] method, and the 6-311+G(3df) basis set was used throughout. Local minima were confirmed by harmonic frequency analyses. The complete basis set (CBS-QB3) method[20] was used for the calculation of accurate relative energies. All calculations were performed using the *Gaussian 03* software package.[21]

RESULTS AND DISCUSSION

General Properties of $OP(N_3)_3$ and $SP(N_3)_3$. Solid $OP(N_3)_3$ and $SP(N_3)_3$ melt at 22 and −30 °C, respectively. The higher melting point of $OP(N_3)_3$ probably indicates stronger intermolecular interactions in the solid state. The colorless liquids at room temperature exhibit low vapor pressures of less than 1 mbar. Small amounts of the samples can be transferred by distillation of the liquid at room temperature on a vacuum line without any decomposition. They can be stored in closed glass vessels at 0 °C for several months.

Vibrational Spectroscopy. The IR (Ar matrix and gas phase) and Raman (solid) spectra of $OP(N_3)_3$ are shown in Figure 1. Observed frequencies are listed in Table 1 and compared to calculated fundamental frequencies at the B3LYP/6-311+G(3df) level of theory. In general, the IR and Raman spectra of the neat sample are consistent with the previously reported spectra measured in concentrated solutions.[4] The presence of three covalently bonded azido ligands in the molecule leads to N_3 in-phase and out-of-phase vibrational modes, which can be clearly distinguished in the Ar-matrix IR and Raman spectra. In the Ar-matrix spectra, the main bands are accompanied by several bands, which may arise from either different matrix sites or the presence of different conformers. When a gaseous mixture of $OP(N_3)_3$/Ar (ca. 1: 1000) at about 1 mbar was heated to about 500 °C prior to its deposition, its matrix IR spectrum revealed no decomposition of the azide and also no change of the relative intensities of the bands, indicating that the splittings of the fundamentals in the

dx.doi.org/10.1021/ic201802x |*Inorg. Chem.* 2011, 50, 11235–11241

Table 1. Experimental and Calculated Vibrational Frequencies (cm^{-1}) of $OP(N_3)_3$

experimental[a]					
IR		Raman[c]	calculated (IR) [Raman][d]		
vapor (298 K)	Ar matrix (16 K)[b]	solid (77 K)	syn (C_3)	anti (C_s)	approximate description of the mode for C_3 symmetry
2193 m, sh	2190.0 m	2201 vs	2309 (52) [147]	2312 (4) [216]	A, ν_1, $\nu_{as}(N_3)$, in-phase
2169 vs	2172.4 vs	2181 sh/2173 s	2293 (928) [66]	2293 (1306) [38]	E, ν_{10}, $\nu_{as}(N_3)$, out-of-phase
				2278 (738) [81]	
1316 m	1311.5 w	1312 m	1289 (149) [4]	1313 (169) [5]	A, ν_2, ν(PO)
		1264 s	1362 (4) [26]	1371 (29) [33]	A, ν_3, $\nu_s(N_3)$, in-phase
1254 s	1258.7 vs		1324 (525) [2]	1333 (632) [1]	E, ν_{11}, $\nu_s(N_3)$, out-of-phase
				1329 (353) [4]	
792 s	781.2 s	787 m	778 (249) [2]	780 (180) [1]	E, ν_{12}, $\nu_{as}(PN_3)$
				757 (242) [1]	
	748.3 w	746 s/734 s	739 (36) [12]	721 (26) [10]	A, ν_4, $\nu_s(PN_3)$
618 w, br	630.6 m	626 w	630 (130) [3]	642 (141) [2]	E, ν_{13}, $\delta(N_3)$, out-of-phase, in plane
				602 (123) [4]	
	598.0 vw	596 m	593 (6) [<1]	593 (16) [<1]	A, ν_5, $\delta(N_3)$, in-phase, out of plane
			589 (3) [<1]	585 (2) [<1]	E, ν_{14}, $\delta(N_3)$, out-of-phase, out of plane
				577 (<1) [<1]	
		536 s	540 (1) [19]	545 (1) [21]	A, ν_6, $\delta(N_3)$, in-phase, in plane
417 w		413 m	416 (39) [1]	416 (42) [<1]	E, ν_{15}, δ(OPN), out-of-phase
				404 (29) [<1]	
		392 w/376 m	362 (1) [3]	373 (4) [3]	A, ν_7, δ(NPN), in-phase
		298 s/278 m	287 (<1) [1]	285 (1) [1]	E, ν_{16}, δ(NPN), out-of-phase
				282 (1) [4]	
			141 (<1) [5]	155 (4) [5]	A, ν_8, δ(PNN), in-phase
			127 (3) [6]	131 (1) [4]	E, ν_{17}, δ(PNN), out-of-phase
				98 (<1) [3]	
			48 (<1) [1]	52 (<1) [2]	A, ν_9, τ, in-phase
			18 (<1) [7]	29 (<1) [3]	E, ν_{18}, τ, out-of-phase
				28 (<1) [9]	

[a] Experimental band positions and intensities: vs, very strong; s, strong; m, medium strong; w, weak; vw, very weak; sh, shoulder. [b] Only the band positions of the most intense matrix sites are given. [c] Splittings of the Raman bands might be caused by deviation from C_3 symmetry in the solid state. [d] B3LYP/6-311+G(3df) level of theory; IR intensities (km mol^{-1}) in parentheses and Raman intensities ($Å^4$ amu^{-1}) in square brackets. For molecular structures of the two calculated conformers, see Figure S2 in the Supporting Information.

Ar-matrix spectrum are due to different matrix sites. Thus, the assignment given in Table 1 is based on the theoretically predicted frequencies for the most stable C_3-symmetrical conformer. Splittings are also observed for some Raman bands, which might be caused by deviation of the molecule from C_3 symmetry in the solid state.

As can be seen in Table 1, the PO stretching vibration is calculated (1289 cm^{-1}) to be lower in frequency than the two symmetric in-phase and out-of-phase N_3 stretches (1362 and 1324 cm^{-1}, respectively). However, the assignment of the higher IR (1316 cm^{-1}; Raman 1312 cm^{-1}) band to ν(PO) is ascertained by its negligible $^{14/15}N$ isotopic shift (Figure S1 in the Supporting Information), while a large shift of 21 cm^{-1} occurred for the band at 1254 cm^{-1}. Apart from these two, the observed band positions and intensities are in good agreement with the calculated data. The descriptions of the vibrational modes given in Table 1 have been deduced from the predicted displacement vectors.

The IR (Ar matrix and gas phase) and Raman (solid) spectra of $SP(N_3)_3$ are shown in Figure 2. The two strongest bands in the gas-phase IR spectrum are located at 2162 and 1246 cm^{-1} and assigned to the antisymmetric and symmetric out-of-phase stretches of the three azido ligands, respectively. Both bands exhibit shoulders at higher frequencies, which correspond to the two weaker in-phase N_3 stretches. Compared to the gas-phase IR spectrum of the precursor $SPCl_3$ (ν(PS) = 769 cm^{-1} and ν(PCl) = 548 cm^{-1}), the two additional strong bands of $SP(N_3)_3$ in the gas-phase IR spectrum at 831 and 763 cm^{-1} should be assigned to $\nu(PN_3)$ and ν(PS), respectively. However, both bands feature $^{14/15}N$ isotopic shifts of 5 and 10 cm^{-1} (Figure S3 in the Supporting Information), respectively, indicating a strong vibrational coupling between them, and the band with the smaller $^{14/15}N$ isotopic shift at 831 cm^{-1} is more reasonably assigned to ν(PS). Consistent with the calculations, they appeared as weak bands at 825 and 757 cm^{-1} in the Raman spectrum of the solid. Similar to $OP(N_3)_3$, the main bands in the Ar-matrix IR spectrum of $SP(N_3)_3$ have several matrix site splittings (Figure 2), and we found no convincing evidence for the presence of a second conformer.

dx.doi.org/10.1021/ic201802x |*Inorg. Chem.* 2011, 50, 11235–11241

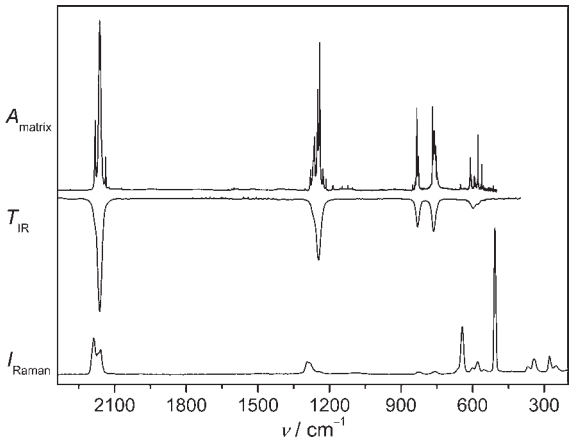

Figure 2. Upper trace: IR spectrum of $SP(N_3)_3$ isolated in an Ar matrix at 16 K (absorbance *A*, resolution 0.25 cm^{-1}). Middle trace: IR spectrum of gaseous $SP(N_3)_3$ at 298 K (transmission *T*, resolution 2 cm^{-1}). Lower trace: Raman spectrum of solid $SP(N_3)_{32}$ at 77 K (Raman intensity *I*, resolution 2 cm^{-1}).

The Raman spectrum of solid $SP(N_3)_3$ shows a very strong, sharp band at 507 cm^{-1}, while no corresponding IR band appeared in this region. The assignment of this band was confirmed with the aid of DFT calculations (Table 2), which predicted a very strong Raman band at 504 cm^{-1}, and it can be assigned to a coupled vibration of $\nu_s(PN_3)$ and $\delta(N_3)$ according to the calculated displacement vectors.

Single-Crystal X-ray Diffraction. Both triazides crystallized in the monoclinic space group $P12_1/c_1$ with four molecules per unit cell. Crystallographic details are given in Table 3. Their molecular structures are shown in Figure 3, and the structural parameters are collected in Table 4.

The three azido ligands in $OP(N_3)_3$ are arranged in a propeller-like fashion. However, they adopt very different dihedral angles with the respective OPN planes (Table 4), which is in contrast to the structure of the related triazide $Sb(N_3)_3$, where all three azido ligands are antiperiplanar to the lone pair of the central antimony atom with perfect C_3 symmetry.[7a] The values for the dihedral angles O−P−N4−N5 [38.68(12)°] and O−P−N7−N8 [0.64(12)°] are very different from that of the

Table 2. Experimental and Calculated Vibrational Frequencies (cm^{-1}) of $SP(N_3)_3$

experimental[a]					
IR		Raman[c]	calculated (IR) [Raman][d]		
vapor (298 K)	Ar matrix (16 K)[b]	solid (77 K)	syn (C_3)	anti (C_s)	approximate description of the mode for C_3 symmetry
2186 w, sh	2181.6 m	2188 vs	2300 (14) [145]	2301 (37) [203]	A, ν_1, $\nu_{as}(N_3)$, in-phase
2162 vs	2163.3 vs	2169 sh/2159 s	2286 (939) [65]	2286 (1241) [37]	E, ν_{10}, $\nu_{as}(N_3)$, out-of-phase
				2269 (738) [96]	
1271 sh	1279.7 w	1293 vs/1283 sh	1356 (<1) [21]	1361 (38) [24]	A, ν_2, $\nu_s(N_3)$, in-phase
1246 vs	1240.7 vs	1241 w	1326 (465) [2]	1333 (503) [2]	E, ν_{11}, $\nu_s(N_3)$, out-of-phase
				1304 (367) [11]	
831 s	834.1 s	825 w	807 (248) [1]	816 (265) [1]	A, ν_3, ν(PS) + $\nu_s(PN_3)$
763 s	768.3 s	757 w	743 (157) [1]	746 (128) [1]	E, ν_{12}, $\nu_{as}(PN_3)$
				722 (140) [<1]	
	651.4 vw	661 w/643 s	646 (4) [9]	667 (25) [7]	A, ν_4, ν(PS) + $\delta(N_3)$, in-phase, in plane
598 w	609.4 m	601 w	606 (104) [5]	612 (124) [2]	E, ν_{13}, $\delta(N_3)$, out-of-phase, in plane
				589 (16) [<1]	
577 vw	578.1 w	579 m	586 (4) [<1]	581 (43) [1]	A, ν_5, $\delta(N_3)$, in-phase, out-of-plane
	555.0 vw	552 w	583 (5) [<1]	578 (41) [4]	E, ν_{14}, $\delta(N_3)$, out-of-phase, out of plane
				573 (<1) [<1]	
		507 vs	504 (2) [37]	504 (1) [39]	A, ν_6, $\nu_s(PN_3)$ + $\delta(N_3)$, in-phase, in plane
		369 w	350 (18) [1]	368 (19) [2]	E, ν_{15}, δ(NPN), out-of-phase
				358 (21) [1]	
		343 m	338 (4) [4]	309 (4) [1]	A, ν_7, δ(NPN), in-phase
		287 m/252 w	260 (<1) [<1]	264 (1) [1]	E, ν_{16}, δ(SPN), out-of-phase
				246 (<1) [5]	
			132 (<1) [7]	122 (1) [7]	A, ν_8, δ(PNN), in-phase
			109 (1) [7]	117 (<1) [2]	E, ν_{17}, δ(PNN), out-of-phase
				98 (<1) [4]	
			48 (<1) [<1]	47 (<1) [2]	A, ν_9, τ, in-phase
			15 (<1) [7]	29 (<1) [8]	E, ν_{18}, τ, out-of-phase
				23 (<1) [3]	

[a] Experimental band positions and intensities: vs, very strong; s, strong; m, medium strong; w, weak; vw, very weak; sh, shoulder. [b] Only the band positions of the most intense matrix sites are given. [c] The splittings of the Raman bands might be caused by deviation from C_3 symmetry in the solid state. [d] B3LYP/6-311+G(3df) level of theory; IR intensities (km mol^{-1}) in parentheses and Raman intensities ($Å^4$ amu^{-1}) in square brackets. For molecular structures of the two calculated conformers, see Figure S2 in the Supporting Information.

dx.doi.org/10.1021/ic201802x |*Inorg. Chem.* 2011, 50, 11235–11241

Table 3. Summary of Crystal Data and Refinement Results for $OP(N_3)_3$ and $SP(N_3)_3$

chemical formula	N_9OP	N_9PS
cryst syst	monoclinic	monoclinic
space group	$P12_1/c_1$ (No. 14)	$P12_1/c_1$ (No. 14)
a (Å)	7.0591(4)	6.1031(5)
b (Å)	12.1904(5)	15.5542(10)
c (Å)	7.7482(4)	7.6411(5)
α (deg)	90	90
β (deg)	111.918(6)	97.077(8)
γ (deg)	90	90
V (Å^3)	618.56(6)	719.84(9)
Z (molecules per unit cell)	4	4
mol wt	173.06	189.12
calcd density (g cm^{-3})	1.858	1.745
T (K)	140(2)	140(2)
μ (mm^{-1})	0.400	0.621
R1[a]	0.0254	0.0299
wR2[b]	0.0684	0.0734

[a] R1 is defined as $\Sigma||F_o| - |F_c||/\Sigma|F_o|$ for $I > 2\sigma(I)$. [b] wR2 is defined as $[\Sigma[w(F_o^2 - F_c^2)^2]/\Sigma w(F_o^2)^2]^{1/2}$ for $I > 2\sigma(I)$.

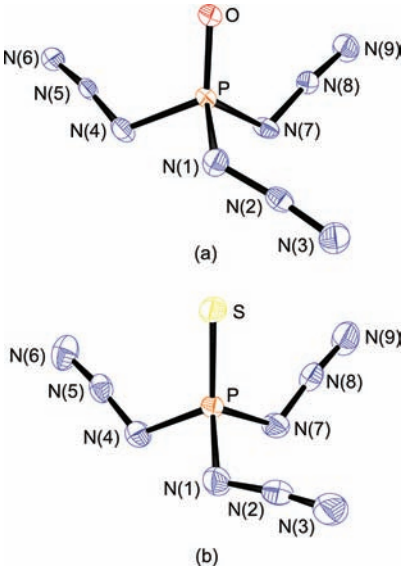

Figure 3. Molecular structures of $OP(N_3)_3$ (a) and $SP(N_3)_3$ (b). Thermal ellipsoids are drawn at the 50% probability level.

O−P−N1−N2 angle [−103.46(11)°], indicating the presence of significant intermolecular contacts.

The packing diagram for $OP(N_3)_3$ is shown in Figure 4. Intermolecular interactions are clearly evidenced by the short O···N_β (N2) distance of 2.875 Å, which is much shorter than the sum of the van der Waals radii of nitrogen (1.55 Å) and oxygen (1.52 Å).[22] The two equal O···N_β interactions between two adjacent molecules form molecular pairs, and their P═O bonds are antiparallel (Figure 4), indicating some dipole−dipole interactions. The other two azido ligands do not participate in such bridging interactions. The intermolecular O···N_β interactions account for the nonequivalence of the three azido ligands of $OP(N_3)_3$ in the solid state, which also explains the above-mentioned

Table 4. Calculated and Experimental Structural Parameters of $OP(N_3)_3$ and $SP(N_3)_3$

	$OP(N_3)_3$			$SP(N_3)_3$		
	calculated[a]			calculated[a]		
parameters[b]	syn	anti	XRD	syn	anti	XRD
R(P−O/S)	1.461	1.456	1.4591(9)	1.914	1.904	1.9025(6)
R(P−N1)	1.682	1.689	1.6647(11)	1.695	1.699	1.6785(16)
R(P−N4)	1.682	1.684	1.6686(11)	1.695	1.700	1.6822(14)
R(P−N7)	1.682	1.684	1.6731(11)	1.695	1.700	1.6797(14)
R(N1−N2)	1.234	1.233	1.2401(16)	1.232	1.234	1.247(2)
R(N2−N3)	1.120	1.121	1.1212(16)	1.120	1.121	1.114(2)
R(N4−N5)	1.234	1.233	1.2533(15)	1.232	1.231	1.244(2)
R(N5−N6)	1.120	1.120	1.1154(15)	1.120	1.121	1.119(2)
R(N7−N8)	1.234	1.233	1.2451(15)	1.232	1.231	1.248(2)
R(N8−N9)	1.120	1.120	1.1163(15)	1.120	1.121	1.113(2)
∠(N1PO/S)	116.9	110.5	117.83(5)	118.3	112.3	120.63(6)
∠(N4PO/S)	116.9	118.4	116.01(5)	118.3	119.6	117.60(6)
∠(N7PO/S)	116.9	118.4	115.71(5)	118.3	119.6	116.37(6)
∠(PN1N2)	119.5	121.5	120.32(9)	119.8	120.4	116.84(12)
∠(PN4N5)	119.5	119.5	117.58(8)	119.8	119.8	116.66(12)
∠(PN7N8)	119.5	119.5	117.57(9)	119.8	119.8	117.47(12)
∠(N1N2N3)	173.8	174.2	172.98(12)	174.3	174.1	173.40(18)
∠(N4N5N6)	173.8	174.0	172.78(12)	174.3	174.7	173.87(17)
∠(N7N8N9)	173.8	174.0	173.38(13)	174.3	174.7	174.33(19)
∠(N1PN4)	101.1	105.7	95.44(6)	99.3	103.6	93.14(7)
∠(N1PN7)	101.1	105.7	104.18(5)	99.3	103.6	100.47(8)
∠(N4PN7)	101.1	96.3	105.01(6)	99.3	95.1	104.88(8)
ϕ(N2N1PO/S)	−38.9	180.0	−103.46(11)	−31.3	180.0	−67.12(16)
ϕ(N5N4PO/S)	−38.9	−32.3	38.68(12)	−31.3	−24.1	26.89(16)
ϕ(N8N7PO/S)	−38.9	−32.3	0.64(12)	−31.3	−24.1	−9.68(15)

[a] At the B3LYP/6-311+G(3df) level of theory. For molecular structures of the two calculated conformers, see Figure S2 in the Supporting Information. [b] Bond lengths and angles are given in Å and deg, respectively; for labeling of atoms, see Figure 3.

larger deviation of the involved azido ligand (N1N2N3) from a synperiplanar orientation to the P═O bond [ϕ(OPN1N2) = −103.46(11)°]. The relative ease in changing the conformation is also supported by the theoretical calculations, which predicted two stable conformers (see below) with an energy difference of merely 1.7 kJ mol^{-1} (CBS-QB3).

The $SP(N_3)_3$ molecule most likely represents a C_3-symmetric structure. The three azido ligands are arranged in a syn conformation with respect to the P═S bond, and the values for the S−P−N1−N2, S−P−N4−N5, and S−P−N7−N8 dihedral angles are −67.12(16), +26.89(16), and −9.68(15)°, respectively. The packing diagram for $SP(N_3)_3$, shown in Figure 5, reveals no noticeable intermolecular interactions.

The replacement of oxygen by sulfur in these triazides mainly elongates the P−N bond lengths, widens the NPO/S angles, and compresses the NPN angles (Table 4); these features can be explained by a reduced positive charge of the central phosphorus atom and an increased space requirement of the larger sulfur atom in $SP(N_3)_3$.

Quantum Chemical Calculations. The structures of $OP(N_3)_3$ and $SP(N_3)_3$ were optimized at the B3LYP/6-311+G(3df) level of theory, and their relative energies were further calculated

dx.doi.org/10.1021/ic201802x |Inorg. Chem. 2011, 50, 11235–11241

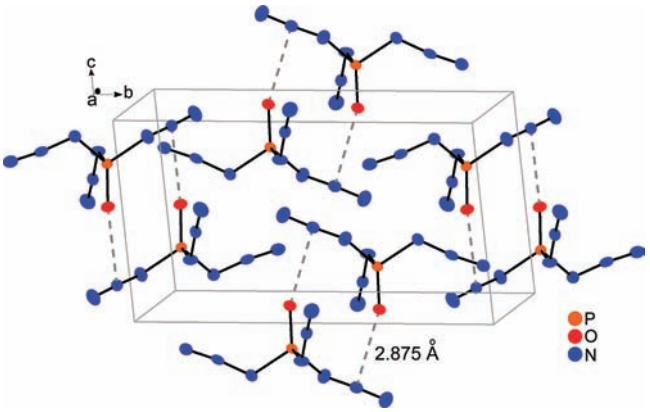

Figure 4. Packing diagram of $OP(N_3)_3$ along the *a* axis showing the intermolecular $O\cdots N_\beta$ bridges.

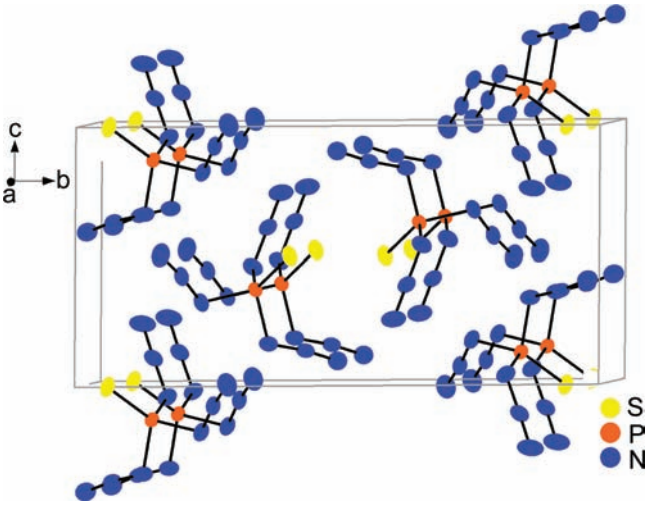

Figure 5. Packing diagram of $SP(N_3)_3$ along the *a* axis.

using the more reliable CBS-QB3 methods. Two local minima were found for both compounds and shown in Figure S2 in the Supporting Information; their structural parameters are collected in Table 4.

The two conformers were calculated (CBS-QB3) to have very similar energies and differ by merely 1.7 and 4.2 kJ mol^{-1} for $OP(N_3)_3$ and $SP(N_3)_3$, respectively. The more stable form for both compounds is the C_3-symmetric syn conformer, where the three azido ligands are in a synperiplanar orientation with respect to the P═O [ϕ(N2N1PO) = −38.9°] and P═S [ϕ(N2N1PS) = −31.3°] bonds, respectively. The less stable anti conformers have C_s symmetry, and one of the azido ligands is in an anti orientation, while the other two are in a synperiplanar orientation [ϕ(N2N1PO) = −32.3°; ϕ(N2N1PS) = −24.1°] to the P═O/S bonds. The preference of the syn conformation can be partially attributed to electronic stabilizing $n_\sigma(N_\alpha) \rightarrow \sigma^*(P{=}O/S)$ interactions, which result in slightly longer P═O/S bonds in the syn conformers [$OP(N_3)_3$ = 1.461 Å; $SP(N_3)_3$ = 1.914 Å] compared to those in the anti conformers [$OP(N_3)_3$ = 1.456 Å; $SP(N_3)_3$ = 1.904 Å]. However, considering the rather small energy differences between the two conformers for both triazides, any packing effects in the solid state can easily deform their structures from the ideal C_3 or C_s symmetry.

CONCLUSION

Two previously reported explosive triazides of phosphorus(V), $OP(N_3)_3$ and $SP(N_3)_3$, have been prepared and isolated as pure substances. Both compounds can be handled as a liquid at room temperature in a small scale. The two triazides have been characterized by IR (Ar matrix and gas phase) and Raman (solid) spectroscopy, and their structures have been determined by X-ray crystallography. For $OP(N_3)_3$, two azido ligands are in a synperiplanar orientation to the P═O bond, while the third one is in an antiperiplanar orientation. Such a strong deviation from the expected ideal C_3 symmetry in the solid is attributed to strong $O\cdots N_\beta$ interactions between the two ajacent molecules. For $SP(N_3)_3$, the three azido ligands are all in a synperiplanar oritentation to the P═S bond. Its solid-state structure is also slightly deviated from C_3 symmetry. Two conformers, syn and anti, were calculated to be stable minima and have very similar energies, The preference of the syn conformation was explained by electronic stabilizing $n_\sigma(N_\alpha) \rightarrow \sigma^*(P{=}O/S)$ interactions.

ASSOCIATED CONTENT

Supporting Information. Gas-phase IR spectra of $^{15}N_2$-labeled $OP(N_3)_3$ and $SP(N_3)_3$, calculated structures of two conformers of $OP(N_3)_3$ and $SP(N_3)_3$, and X-ray crystallographic files in CIF format of the structure determination of $OP(N_3)_3$ and $SP(N_3)_3$. This material is available free of charge via the Internet at http://pubs.acs.org.

AUTHOR INFORMATION

Corresponding Author

*E-mail: zeng@uni-wuppertal.de.

ACKNOWLEDGMENT

This work was supported by the Deutsche Forschungsgemeinschaft (DFG) and the Fonds der Chemischen Industrie.

REFERENCES

(1) For example, see: (a) Lang, S.; Murphy, J. A. *Chem. Soc. Rev.* **2006**, *35*, 146–156. (b) Bräse, S.; Gil, C.; Knepper, K.; Zimmermann, V. *Angew. Chem., Int. Ed.* **2005**, *44*, 5188–5240. (c) Tornieporth-Oetting, I. C.; Klapötke, T. M. *Angew. Chem., Int. Ed. Engl.* **1995**, *34*, 511–520.

(2) For example, see: (a) Knapp, C.; Passmore, J. *Angew. Chem., Int. Ed.* **2004**, *43*, 834–836. (b) Göbel, M.; Karaghiosoff, K.; Klapötke, T. M. *Angew. Chem., Int. Ed.* **2006**, *45*, 6037–6040. (c) Haiges, R.; Boatz, J. A.; Christe, K. O. *Angew. Chem., Int. Ed.* **2010**, *49*, 8008–8012.

(3) Evers, J.; Göbel, M.; Krumm, B.; Martin, F.; Medvedyev, S.; Oehlinger, G.; Steemann, F. X.; Troyan, I.; Klapötke, T. M.; Eremets, M. I. *J. Am. Chem. Soc.* **2011**, *133*, 12100–12105.

(4) Buder, W.; Schmidt, A. *Z. Anorg. Allg. Chem.* **1975**, *415*, 263–267.

(5) Dillon, K. B.; Platt, A. W. G.; Waddington, T. C. *Inorg. Nucl. Chem. Lett.* **1978**, *14*, 511–513.

(6) Götz, N.; Herler, S.; Mayer, P.; Schulz, A.; Villinger, A.; Weigand, J. J. *Eur. J. Inorg. Chem.* **2006**, 2051–2057.

(7) (a) Haiges, R.; Vij, A.; Boatz, J. A.; Schneider, S.; Schroer, T.; Gerken, M.; Christe, K. O. *Chem.—Eur. J.* **2004**, *10*, 508–517. (b) Klapötke, T. M.; Geissler, P. *J. Chem. Soc., Dalton Trans.* **1995**, 3365–3366.

(8) (a) Haiges, R.; Boatz, J. A.; Vij, A.; Vij, V.; Gerken, M.; Schneider, S.; Schroer, T.; Yousufuddin, M.; Christe, K. O. *Angew. Chem., Int. Ed.* **2004**, *43*, 6676–6680. (b) Karaghiosoff, K.; Klapötke, T. M.; Krumm, B.; Nöth, H.; Schütt, T.; Suter, M. *Inorg. Chem.* **2002**, *41*, 170–179.

(9) (a) Schulz, S.; Lyhs, B.; Jansen, G.; Bläser, D.; Wölper, C. *Chem. Commun.* **2011**, *47*, 3401–3403. (b) Klapötke, T. M.; Schulz, A.; McNamara, J. *J. Chem. Soc., Dalton Trans.* **1996**, 2985–2987.

(10) (a) Villinger, A.; Schulz, A. *Angew. Chem., Int. Ed.* **2010**, *49*, 8017–8020. (b) Klapötke, T. M.; Schulz, A. *Main Group Met. Chem.* **1997**, *20*, 325–338.

(11) For example, see: (a) Zeng, X. Q.; Beckers, H.; Bernhardt, E.; Willner, H. *Inorg. Chem.* **2011**, *50*, 8679–8684. (b) Zeng, X. Q.; Gerken, M.; Beckers, H.; Willner, H. *Inorg. Chem.* **2010**, *49*, 9694–9699. (c) Zeng, X. Q.; Gerken, M.; Beckers, H.; Willner, H. *Inorg. Chem.* **2010**, *49*, 3002–3010.

(12) For example, see: (a) Zeng, X. Q.; Beckers, H.; Willner, H. *Angew. Chem., Int. Ed.* **2011**, *50*, 482–485. (b) Zeng, X. Q.; Beckers, H.; Willner, H.; Stanton, J. F. *Angew. Chem., Int. Ed.* **2011**, *50*, 1720–1723. (c) Zeng, X. Q.; Beckers, H.; Willner, H. *Angew. Chem., Int. Ed.* **2009**, *48*, 4828–4831.

(13) Gombler, W.; Willner, H. *J. Phys. E.: Sci. Instrum.* **1987**, *20*, 1286.

(14) *CrysAlisPro*, version 1.171.33.42; Oxford Diffraction Ltd.: Oxford, U.K., 2010.

(15) Farrugia, L. J. *WinGX v1.64.05—An Integrated System of Windows Programs for the Solution, Refinement and Analysis of Single Crystal X-ray Diffraction Data*; University Glasgow: Glasgow, Scotland, 2003 (*J. Appl. Crystallogr.* **1999**, *32*, 837−838).

(16) Sheldrick, G. M. *SHELXS-97, Program for Crystal Structure Solution*; Universität Göttingen, Göttingen, Germany, 1997.

(17) Sheldrick, G. M. *SHELXL-97, Program for Crystal Structure Refinement*; Universität Göttingen: Göttingen, Germany, 1997.

(18) Brandenburg, K. *Diamond*, version.2.1e; Crystal Impact GbR: Bonn, Germany, 2001.

(19) Becke, A. D. *J. Chem. Phys.* **1993**, *98*, 5648–5652.

(20) Montgomery, J. A., Jr.; Frisch, M. J.; Ochterski, J. W.; Petersson, G. A. *J. Chem. Phys.* **2000**, *112*, 6532–6542.

(21) Frisch, M. J.; Trucks, G. W.; Schlegel, H. B.; Scuseria, G. E.; Robb, M. A.; Cheeseman, J. R.; Montgomery, J. A., Jr.; Vreven, T.; Kudin, K. N.; Burant, J. C.; Millam, J. M.; Iyengar, S. S.; Tomasi, J.; Barone, V.; Mennucci, B.; Cossi, M.; Scalmani, G.; Rega, N.; Petersson, G. A.; Nakatsuji, H.; Hada, M.; Ehara, M.; Toyota, K.; Fukuda, R.; Hasegawa, J.; Ishida, M.; Nakajima, T.; Honda, Y.; Kitao, O.; Nakai, H.; Klene, M.; Li, X.; Knox, J. E.; Hratchian, H. P.; Cross, J. B.; Adamo, C.; Jaramillo, J.; Gomperts, R.; Stratmann, R. E.; Yazyev, O.; Austin, A. J.; Cammi, R.; Pomelli, C.; Ochterski, J. W.; Ayala, P. Y.; Morokuma, K.; Voth, G. A.; Salvador, P.; Dannenberg, J. J.; Zakrzewski, V. G.; Dapprich, S.; Daniels, A. D.; Strain, M. C.; Farkas, O.; Malick, D. K.; Rabuck, A. D.; Raghavachari, K.; Foresman, J. B.; Ortiz, J. V.; Cui, Q.; Baboul, A. G.; Clifford, S.; Cioslowski, J.; Stefanov, B. B.; Liu, G.; Liashenko, A.; Piskorz, P.; Komaromi, I.; Martin, R. L.; Fox, D. J.; Keith, T.; Al-Laham, M. A.; Peng, C. Y.; Nanayakkara, A.; Challacmobe, M.; Gill, P. M. W.; Johnson, B.; Chen, W.; Wong, M. W.; Gonzalez, C.; Pople, J. A. *Gaussian 03*, revison D.01; Gaussian, Inc.: Wallingford, CT, 2003.

(22) Bondi, A. *J. Phys. Chem.* **1964**, *68*, 441–451.